Pharm Res (2010) 27:2307–2316
DOI 10.1007/s11095-010-0179-6

RESEARCH PAPER

PAMAM-Camptothecin Conjugate Inhibits Proliferation and Induces Nuclear Fragmentation in Colorectal Carcinoma Cells

Giridhar Thiagarajan • Abhijit Ray • Alexander Malugin • Hamidreza Ghandehari

Received: 30 November 2009 / Accepted: 24 May 2010 / Published online: 15 June 2010

ABSTRACT

Purpose To synthesize and characterize a poly (amido amine) dendrimer-camptothecin (PAMAM-CPT) conjugate and evaluate its activity on human colorectal carcinoma cells (HCT-116).

Methods The attachment of CPT to amine-terminated PAMAM was facilitated through a succinic acid-glycine linker. The conjugate was characterized for absence of small molecular weight impurities, size and drug content. Stability of the conjugate in PBS and growth media and its *in vitro* activity on HCT-116 were studied. Cell cycle arrest and nuclear fragmentation upon PAMAM-CPT treatment were investigated.

Results The conjugate was stable under physiological pH (7.4) in PBS and in growth media (with 10% FBS) with minimal release of 4% and 6% drug, respectively, at 48 h. PAMAM-CPT inhibited proliferation of HCT-116 cells with an IC50 value of 1.6 ± 0.3 μM. The conjugate induced signs of cell cycle arrest with up to 68% of cells blocked in the G_2 phase. Confocal images of cells treated with PAMAM-CPT suggest nuclear fragmentation and formation of apoptotic bodies.

Conclusions Results show that the PAMAM-CPT conjugate was active against colorectal cancer cells *in vitro*, inhibiting their growth and inducing nuclear fragmentation. Coupled with the ability to target macromolecular therapeutics to tumors, this conjugate shows promise for cancer chemotherapy.

KEY WORDS PAMAM dendrimer · camptothecin · drug delivery · colorectal cancer

ABBREVIATIONS

ATCC	American type culture collection
BOC	tert-Butyloxycarbonyl
CCK	cell counting kit
CPT	camptothecin
DAPI	4′, 6-diamidino-2-phenylindole
DCM	dichloromethane
DI	deionized
DIPC–N	N'–diisopropyl carbodiimide
DIPEA–N	N–diisopropyl ethylamine
DLS	dynamic light scattering
DMAP	4-dimethyl amino pyridine
DMSO	dimethyl sulfoxide
DNA	deoxyribonucleic acid
EDC (m)	1-[3-(dimethyl amino) propyl]-3 ethyl carbodiimide methiodide
EPR	enhanced permeability and retention
FBS	fetal bovine serum
FPLC	fast protein liquid chromatography
G4.0	Generation 4.0
HPLC	high performance liquid chromatography
IC_{50}	half maximal inhibitory concentration
MW	molecular weight
MWCO	molecular weight cutoff
NHS-s	N-hydroxy sulfosuccinimide sodium salt
P-gp	permeability glycoprotein

Electronic supplementary material The online version of this article (doi:10.1007/s11095-010-0179-6) contains supplementary material, which is available to authorized users.

G. Thiagarajan • H. Ghandehari
Department of Bioengineering, University of Utah
Salt Lake City, Utah 84108, USA

G. Thiagarajan • A. Ray • A. Malugin • H. Ghandehari
Utah Center for Nanomedicine, Nano Institute of Utah
University of Utah
Salt Lake City, Utah 84108, USA

A. Ray • A. Malugin • H. Ghandehari (✉)
Department of Pharmaceutics and Pharmaceutical Chemistry
University of Utah
Salt Lake City, Utah 84108, USA
e-mail: hamid.ghandehari@pharm.utah.edu

PAMAM	Poly (amido amine)
PBS	phosphate buffered saline
PEG	Poly (ethylene glycol)
RNAse	ribonuclease
SEC	size exclusion chromatography
TFA	trifluoroacetic acid
THF	tetrahydrofuran
TLC	thin layer chromatography
UV	ultraviolet
WST	water-soluble tetrazolium salt
Wt	weight

INTRODUCTION

Camptothecin (CPT) is a potent chemotherapeutic drug that is used clinically to treat a variety of malignancies (1). It is a plant alkaloid from the tree *Camptotheca acuminata* which inhibits the DNA enzyme *topoisomerase I*. Like many anti-cancer drugs, CPT is poorly water-soluble, causes systemic toxicity, has low oral bioavailability and is limited by dose-related toxic effects (2). CPT-based delivery systems can provide selective tumor accumulation, increase solubility and efficacy and reduce adverse drug reaction (3). Analogs of CPT such as irinotecan and topotecan are widely used in chemotherapy against colorectal cancers (1) along with other anti-cancer drugs such as 5-fluorouracil and oxaliplatin. Colorectal cancer is among the leading causes of cancer-related deaths (4). These cancers demonstrate minor symptoms reducing the chance of early diagnosis and are present in anatomically inaccessible sites further complicating treatment. Current therapies include surgery assisted by combination chemotherapy (5) and radiation therapy but with only limited benefit during advanced stages of the disease and hepatic metastasis (6).

The central problem in cancer chemotherapy is the severe toxic effects of available drugs to healthy tissue, thus limiting the dosage and causing treatment delays or resulting in termination of therapy. Polymeric conjugates of anti-cancer drugs have shown to be beneficial because they can alter biological distribution, improve therapeutic efficacy, lead to longer retention times, and most importantly reduce systemic toxicity (7). Polymer therapeutics can accumulate passively at the tumor site due to the enhanced permeation and retention (EPR) effect (8) and escape P-gp efflux pumps (9) overcoming multi-drug resistance.

Poly (amido amine) (PAMAM) dendrimers are a unique class of nano-scale polymers with highly defined architecture and multifunctional surface groups that can carry multiple molecular entities (10–12). The physical, chemical and biological characteristics of branched PAMAM dendrimers combined with passive targeting based on nano-dimension mediated EPR effect (11,13) make them useful candidates for targeted delivery of anti-cancer agents. PAMAM dendrimers can increase the solubility of hydrophobic drugs (14–16) and improve translocation across epithelial and endothelial barriers (9,17–20), increasing the oral bioavailability of poorly soluble and poorly bioavailable drugs. We have shown that complexes of PAMAM and CPT analogs improve the trans-epithelial transport and cellular uptake (20) of the drug. It would be desirable to synthesize and characterize covalent conjugates of such systems so that non-specific release in the blood-stream is reduced and release is facilitated at the target site. As a step towards that goal we present here the synthesis, characterization and *in vitro* evaluation of a PAMAM-CPT conjugate.

MATERIALS AND METHODS

Chemicals

Poly (amido amide) (PAMAM) dendrimers of generation 4 (G4.0, MW = 14,214.17) were purchased from Sigma Aldrich (St. Louis, MO). Camptothecin (CPT, MW = 348.35) was purchased from AK Scientific (Mountain View, CA). BOC-Glycine-OH, 4-dimethyl amino pyridine (DMAP), trifluoroacetic acid, N, N'–diisopropyl carbodiimide (DIPC), 1-[3-(dimethyl amino) propyl]–3 ethyl carbodiimide methiodide (EDC (m)), N-hydroxy sulfosuccinimide sodium salt (NHS-s), N, N–diisopropyl ethylamine (DIPEA), succinic anhydride and dimethyl sulfoxide (DMSO) were also purchased from Sigma Aldrich (St. Louis, MO). Silica gel 60 was purchased from Alfa Aesar (Ward Hill, MA). All solvents used in this study were purchased from VWR International (West Chester, PA) and used directly without any further purification unless otherwise mentioned.

Synthesis of PAMAM-CPT

PAMAM-CPT conjugate was obtained in a three-step synthetic procedure as indicated in Scheme 1 and briefly described below.

Glycine-Camptothecin (1a)

BOC-glycine-OH was attached to CPT (4-Ethyl-4-hydroxy-3, 4, 12, 14-tetrahydro-1H-pyrano [3′, 4′: 6, 7] indolizino [1, 2-b] quinoline-3, 14-dione) through an ester bond at 20–OH position similar to a reported procedure (21) with modifications. Briefly, BOC-glycine-OH (1.157 g, 6.61 mM) and CPT (1.150 g, 3.31 mM) were dissolved in 1.2 l of 3:7 mixture of anhydrous dichloromethane (DCM) and anhydrous tetrahydrofuran (THF). The solution was cooled to 0°C with stirring followed by the addition of DMAP (0.808 g,

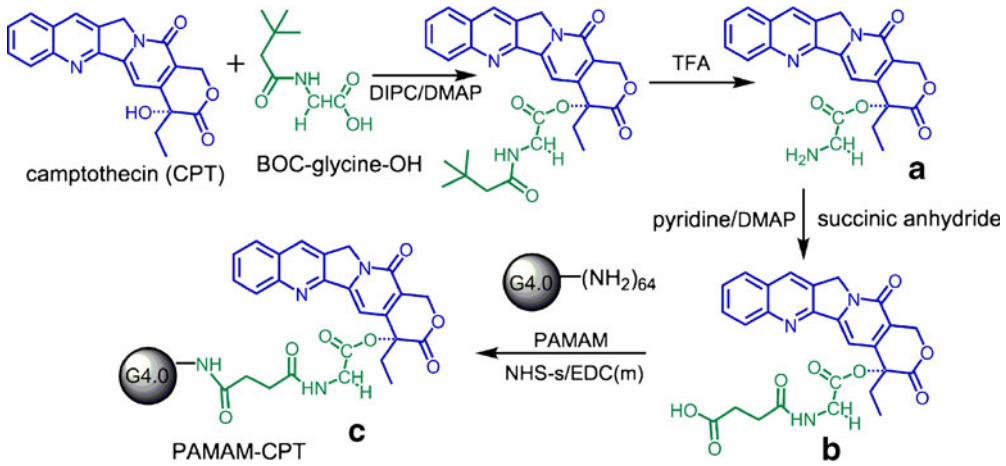

Scheme I Schematics of the three-step synthesis of PAMAM-CPT conjugate. CPT; Spacer (succinic acid-glycine); PAMAM dendrimer. For abbreviations, see abbreviations list.

6.61 mM) and DIPC (0.834 g, 1.023 ml, 6.61 mM) under anhydrous conditions. The temperature was maintained at 0°C for 2 h and then allowed to warm to room temperature with continued stirring overnight. Completion of reaction was monitored by the disappearance of the starting material using thin layer chromatography (eluent—methanol: ethylacetate : 1:19 (v/v)). The product was purified by column chromatography (Silica gel 60) and eluted in 5% methanol in ethyl acetate. The combined organic solvent was concentrated in-vacuo. The concentrated product was dissolved in a 20% solution of TFA (v/v) in anhydrous DCM (100 ml) and stirred for 2–4 h to yield glycine-camptothecin. The acidic solution was neutralized by DIPEA, and the solvent was evaporated under vacuum to give glycine-CPT. The product was confirmed by mass spectroscopy (m/z, M^{+1}) and used for the subsequent reaction without further modification.

Succinic Acid-Glycine-Camptothecin, (S-G-CPT) (1b)

Glycine-CPT (100 mg, 0.247 mM) was dissolved in anhydrous pyridine (20 ml). Succinic anhydride (49.34 mg, 0.493 mM) and catalytic amounts of DMAP were added to the reaction mixture and refluxed at 60°C under overnight stirring. Completion of the reaction was monitored by the disappearance of the starting material on TLC (Eluent—methanol: ethylacetate : 1:9 (v/v)). The solvent was evaporated under vacuum, and then the product was purified by column chromatography (Silica gel 60) and eluted in 10% methanol in ethyl acetate to yield S-G-CPT. The formation of the product was confirmed by mass spectroscopy (m/z, M^{+1}).

G4.0-Succinic Acid-Glycine-Camptothecin, (PAMAM-CPT) (1c)

Succinic acid-Glycine-CPT (34 mg, 67.3 μM) (S-G-CPT) was dissolved in 15 ml of DI water followed by addition of a few drops of DMSO (0.5 ml) to obtain a clear solution. NHS-s (29.25 mg, 134.6 μM) and EDC (m) (40 mg, 134.6 μM) were added sequentially and stirred at room temperature for 5–10 min. Methanol in the G4.0 solution (79.75 mg, 5.6 μM) was evaporated to dryness under vacuum and dissolved in DI water (5 ml) followed by addition of 0.3 ml of DIPEA. This mixture was added to the above aqueous reaction and stirred overnight. Progress of reaction was monitored by TLC. Product was dialyzed (Spectrapor®, MWCO 3500) against DI water to remove small-molecular-weight impurities. The conjugate was purified from residual free drug by size exclusion chromatography using a Superdex 75, HiLoad (16/60) prep grade column (GE Healthcare, Piscataway, NJ). The final product was lyophilized to obtain a powder product.

Characterization of PAMAM-CPT

Size Exclusion Chromatography (SEC) and Dynamic Light Scattering (DLS)

The synthesized PAMAM-CPT conjugate was characterized by obtaining a size exclusion chromatography profile on an Akta FPLC system (GE Healthcare, Piscataway, NJ) with a Sepharose 12 (10/300) column (GE Healthcare, Piscataway, NJ). Phosphate-buffered solution (PBS, pH 7.4) with 1% sodium azide was used as elution solvent. 0.1 ml of a 4 mg/ml solution of PAMAM-CPT was injected into the column after filtering through a 0.2 μm membrane. Ultra-violet (UV) and DLS detections were simultaneously monitored, and conjugate peak was analyzed to determine its hydrodynamic radius using a Quasi-Elastic Light Scattering (QELS, Wyatt Technology Corporation, Santa Barbara, CA) detector, and calculations were performed using the *Astra V* 5.3.4.14 software (Wyatt Technology Corporation, Santa Barbara, CA) with a dn/dc value of 0.134 as projected by the software. Size measurements of the native G4.0 dendrimer were done on samples purchased directly from Sigma (St. Louis, MO).

High Performance Liquid Chromatography (HPLC)

The product was analyzed for the absence of traces of free drug by HPLC using a C18, 5 μm column purchased from Waters (Milford, MA), mobile phase of a mixture of acetonitrile (HPLC grade) and water with 0.14% TFA in the ratio of 27:73. Twenty μl of sample was injected from a filtered 3 mg/ml solution of the PAMAM-CPT conjugate.

UV Spectrometry

Drug loading on the PAMAM dendrimer was determined using a UV-Vis spectrophotometer SpectraMax M2 (Molecular Devices, Sunnyvale, CA). The PAMAM-CPT conjugate was dissolved in DMSO and analyzed for absorbance at 370 nm. The number of CPT molecules conjugated to the PAMAM dendrimer was determined using a standard curve that was plotted based on the free drug's absorbance at different concentrations.

In Vitro Evaluation of PAMAM-CPT

Stability of the Conjugate

The stock solution of the PAMAM-CPT conjugate was prepared in distilled water and filtered through a 0.2 μm membrane. In a typical experiment, 150 μl of the stock solution was added to either PBS or growth media (GM) to make up a final volume of 1,500 μl and a PAMAM-CPT conjugate concentration of 115 μM. The stock volume added was less than 10% of the entire sample. The sample was incubated at 37°C and stirred continuously. Aliquots of 200 μl were taken out at each time point and frozen at –80°C until further investigation. Aliquots were later thawed, and the drug released was extracted into a layer of DCM. The samples were extracted three times with equivalent volume of DCM, solvent evaporated and reconstituted in mobile phase and analyzed by HPLC as mentioned above.

Cell Line

Human colorectal carcinoma cells, HCT-116, were purchased from ATCC (Manassas, VA). Cells (passages 5–25) were grown in McCoy's 5A media modified (ATCC) supplemented with 10% Fetal Bovine Serum (HyClone Laboratories, Ogden UT) in 5% CO_2 incubators at 37°C and were maintained in logarithmic phase throughout all experiments.

Evaluation of Cell Proliferation and Viability

HCT-116 cells were plated in a 96-well plate at a density of 3,000 cells/well and cultured for 40 h before being subject to various treatments. Stock solutions of CPT, S-G-CPT and PAMAM-CPT were made in DMSO and filtered through a 0.2 μm membrane before use. The treatment of various concentration ranges on the cells lasted for 48 h, after which relative number of cells was measured using water-soluble tetrazolium salt, WST-8 [2-(2-methoxy-4nitrophenyl)-3-(4-nitrophenyl)-5-(2,4-disulfophenyl)-2H-tetrazolium, monosodium salt], as a part of the cell counting kit-8 (CCK-8, Dojindo Molecular Technologies, Rockville, MD). G4.0 dendrimers (polymer alone) were tested on cells at concentrations equivalent to polymer content in the conjugate. IC_{50} values (concentration of the sample that killed 50% of the cells relative to control cells) were determined using GraphPad Prism 5.01 software (GraphPad Software, Inc., La Jolla, CA).

Cell Cycle Analysis

Cell cycle progression was monitored by flow cytometry measurement (22). Briefly, 0.5×10^6 cells/well were plated in a 6-well plate and cultured for 24 h, after which they were treated with $3\times IC_{50}$ concentrations of CPT and PAMAM-CPT for 24 h. Cells were fixed in 70% ethanol, and stained with 50 μg/ml propidium iodide (Sigma-Aldrich, St. Louis, MO). Double-stranded RNA was removed enzymatically by incubating stained cells with 10 μg/ml of ribonuclease (RNAse A, Sigma-Aldrich, St. Louis, MO) for 30 min at room temperature. Analysis of DNA content in cells stained with propidium iodide was performed using FACScan (Becton Dickinson, Mountain View, CA). Percentage of cells in each phase of the cell cycle was evaluated using ModFit LT 3.1 software (Verity Software House, Topsham, ME).

Nuclear Fragmentation and Apoptotic Body Formation

Cells cultured on a glass cover slip were treated with CPT and PAMAM-CPT at $3\times IC_{50}$ concentrations for 24 h and later fixed with 4% paraformaldehyde. Fixed cells were stained with DAPI (Santa Cruz Biotechnology, Santa Cruz, CA) and visualized by a confocal laser-scanning microscope, Olympus FluoView FV1000 (Olympus Corp., Center Valley, PA). Single slice images were captured using a 60× oil immersion objective with numerical aperture1.42 and FV10 ASW 1.7 software.

Statistical Analysis

Student's *T*-test was used to analyze the statistical significance between IC_{50} values. Percentages of cell population in different phases of cell cycle were also analyzed by the same test for statistical significance between different treatment groups. Hydrodynamic radii as determined by

DLS for native PAMAM and PAMAM-CPT conjugates were also analyzed for statistical significance. Welch's correction that does not assume equal variance was performed with a two-tailed test. P-values of <0.05 were indicative of statistical difference.

RESULTS AND DISCUSSION

Synthesis and Characterization of PAMAM-CPT

CPT was successfully conjugated to amine-terminated PAMAM dendrimer generation 4 according to procedure described in Scheme 1. The site of attachment on the CPT molecule was the 20–OH group, and it was conjugated with glycine through a biodegradable ester bond as a substrate for *esterases*. The major sub-cellular location of *esterases* is in the lysosomal compartment (23,24) and in liver tissue (24,25), which is the predominant site of colorectal metastasis (26). Native G4.0 PAMAM dendrimers were used since they are effective in permeating across intestinal epithelial monolayers (27) and their complexes with a CPT analog showed increased uptake and transport across Caco-2 cells (20). The glycine spacer was introduced to reduce steric hindrance during attachment of the drug to the dendrimer. Succinic acid was subsequently attached to glycine to enable coupling to the amine–terminated G4.0 PAMAM dendrimer. A glycine-based spacer is also known to influence controlled release of the drug as reported earlier (28) and can prevent premature release in the bloodstream. Another distinct advantage of coupling an amino acid spacer via the hydroxyl group at 20- carbon position of camptothecin is that it stabilizes the lactone ring of the drug (29). This was confirmed by mass spectrometry of glycine-camptothecin (m/z, M^{+1}, 406.0) and succinic acid-glycine-camptothecin (m/z, M^{+1}, 506.1) (see Supplementary Material). Lactone ring-opened form of these intermediate compounds would have an 18 Da difference in mass from the ring-intact form, but only a single peak corresponding to the ring-intact form was observed in the mass spectra, which denotes the absence of ring opening. Lactone ring opening of CPT renders it inactive since it's the active site of CPT that interacts with DNA-*topoisomerase I* covalent complex, ultimately inducing apoptosis (2).

Absence of small molecular weight impurities in the conjugate was confirmed by HPLC and SEC. Chromatograms indicated a single peak corresponding to the polymeric conjugate, and no small molecular impurities were observed. Hydrodynamic radius of the conjugate was determined to be 1.54 ± 0.23 nm using DLS techniques (Table I), and conjugating a small molecular weight drug to PAMAM did not alter its size statistically from the native dendrimer (1.45 ± 0.07 nm). The DLS data corroborated with size exclusion chromatography elution volumes (Table I). Analysis of the conjugate's UV absorption spectra indicated a λ_{max} of 370 nm that corresponds to CPT's absorbance. Drug loading on the PAMAM-CPT conjugate was about 5 wt% (Table I).

Stability in PBS and Growth Media

It is important to study the conjugate's stability profile under physiological conditions (pH 7.4) and in the presence of serum proteins as it helps to better understand the release pattern of CPT from the conjugate. Ester bonds are susceptible to *esterase* activity (30). Although they are relatively stable under neutral pH values, ester bonds are known to hydrolyze under both acidic and basic conditions (31). Stability of the conjugate in both growth media and PBS (pH 7.4) was studied to differentiate breakdown of the conjugate due to hydrolysis or due to the presence of proteins and proteolytic enzymes such as *esterases* and *amidases* in serum. Results (Fig. 1) indicate there is a gradual increase in released drug with time in both PBS and growth media. A maximum 6% of CPT was released under growth media conditions, and 4% was released in PBS over 48 h of incubation at 37°C. The maximum incubation time was kept at 48 h to correlate with the duration that PAMAM-CPT conjugates were incubated with cells during the *in vitro* experiments. The control experiment with free drug (CPT) equivalent to 100% of drug present in the conjugate (Fig. 1) shows the extraction procedure employed was robust and allowed detection of 100% drug if it was released from the conjugate.

Table I Characterization of PAMAM-CPT Conjugate

Sample	SEC elution volume (ml)	Measured radius (nm)	Reported radius (nm)[b]	Drug loading on PAMAM (%)	# of CPT / PAMAM G4.0
PAMAM-CPT	14.0	1.54 ± 0.23[a]	–	4.51 ± 0.1[a]	1.89 ± 0.004[*]
PAMAM (G4.0)	14.1	1.45 ± 0.071[a]	2 (1.5)	–	–

[a] Mean ± standard deviation, $n = 3$; DLS measurements were calculated based on a dn/dc value of 0.134 using *Astra V* 5.3.4.14 software

[b] Reported values (43) are based on size exclusion chromatography (2 nm) and molecular modeling of compact structure (1.5 nm)

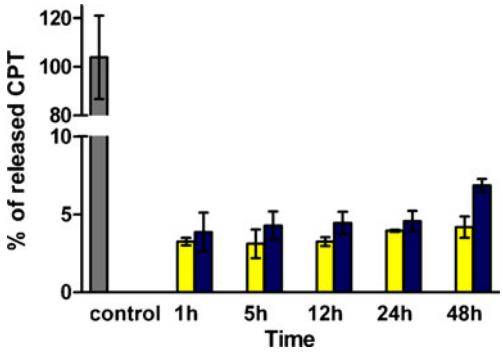

Fig. 1 CPT released from PAMAM-CPT conjugate in PBS (■) and growth media (■). 115 μM of the conjugate was incubated at 37°C, and aliquots were drawn at various time points over 48 h. Samples were later analyzed by HPLC. Control measurement shows bar with 100% equivalent of free CPT. Mean values±S.D. from three independent experiments are presented.

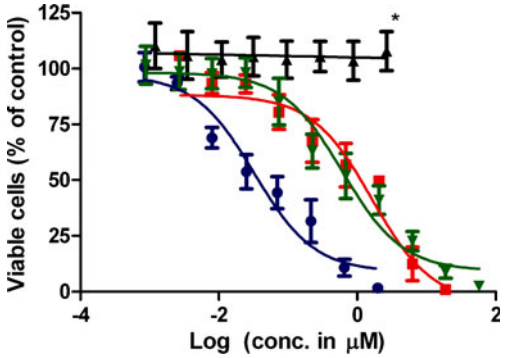

Fig. 2 Toxicity of different forms of CPT on HCT-116 cells. ▲ PAMAM G4.0; ■ PAMAM-CPT; ▼ S-G-CPT; ● CPT. Cells were incubated with various concentrations of drugs for 48 h. Relative cell number was determined by a WST-8 assay. Mean values±S.D. from three independent experiments are presented. * indicates PAMAM G4.0 polymer alone treatment at corresponding conjugate equivalent concentrations.

The slightly higher release (2%) of CPT in growth media compared to PBS may be attributed to the presence of *esterases* in fetal bovine serum. Fetal bovine serum contains growth factors, sugars, hormones, amino acids and enzymes amongst which *esterases* are also present (32). *Esterases* could potentially cleave the ester bond between glycine and camptothecin (21) in the conjugate, causing release of CPT. Previous reports indicate that ester bond breakdown in linear PEG-CPT conjugates (21) has a half life of 40 h in PBS, whereas dendrimer conjugates reported here are relatively stable with a maximum release of 4% at 48 h. This observation suggests a possible role of polymer architecture, accessibility and/or polymer hydration in affecting the stability of these conjugates since the drug and nature of linker bonds between the dendrimer conjugates of CPT and PEG-CPT conjugates mentioned above are essentially the same. Nevertheless, the data indicate that both hydrolysis in buffer and growth media conditions contributed to a minimal release of the drug observed over time, establishing the stability of the conjugate.

Inhibition of Cell Growth

The three analogs (CPT, S-G-CPT, and PAMAM-CPT) inhibited growth of HCT-116 cells (Fig. 2) to different extents. The free drug (CPT) was more active in inhibiting growth of these cells followed by S-G-CPT and PAMAM-CPT. There is a notable 50-fold difference in the toxicity profiles of CPT and PAMAM-CPT as evident from their IC_{50} values (Table II). This difference was expected based on earlier observations (7) that conjugating a drug to a polymeric system results in reduced toxicity based on altered kinetics of drug entry into cell, limited access to sites of toxicity and release profile from the polymer. The difference in IC_{50} values between S-G-CPT (spacer+drug) and PAMAM-CPT is close to 3 times, which seems logical considering the proposed mechanism of drug release by breakdown of the ester bond present between the drug and spacer. The spacer and dendrimer are linked by an amide bond, which is known to be relatively stable and may not affect drug release to a great extent. Also significant to note was that G4.0 (polymer alone) was non-toxic to these cells at concentrations equivalent to that applied as a part of the PAMAM-CPT conjugate (Fig. 2).

It was inevitable to analyze whether the 6% drug released from PAMAM-CPT under growth media conditions in 48 h could contribute to the entire toxicity observed due to conjugate treatment. A corresponding theoretical growth inhibition curve of 6% drug released from the conjugate was constructed to evaluate this effect (data not shown). It was found that the IC_{50} value calculated from this theoretical curve was three times higher than that of the free drug (Table II), implying that a lot more drug needed to be released from the conjugate in order to observe the same magnitude of cytotoxicity as

Table II IC_{50} Values of CPT Analogs

Sample	IC_{50} (in μM)
CPT (Free drug)	0.033 ± 0.005^a
S-G-CPT (Drug + Linker)	0.615 ± 0.066^a
PAMAM-CPT (Conjugate)	1.627 ± 0.305^a
G4 (Polymer alone)	Non-toxic at equivalent concentrations of conjugate treatment

[a] IC_{50} values of CPT, S-G-CPT, and PAMAM-CPT are statistically significant from each other ($P < 0.05$). Mean values+S.D. from three independent experiments are presented

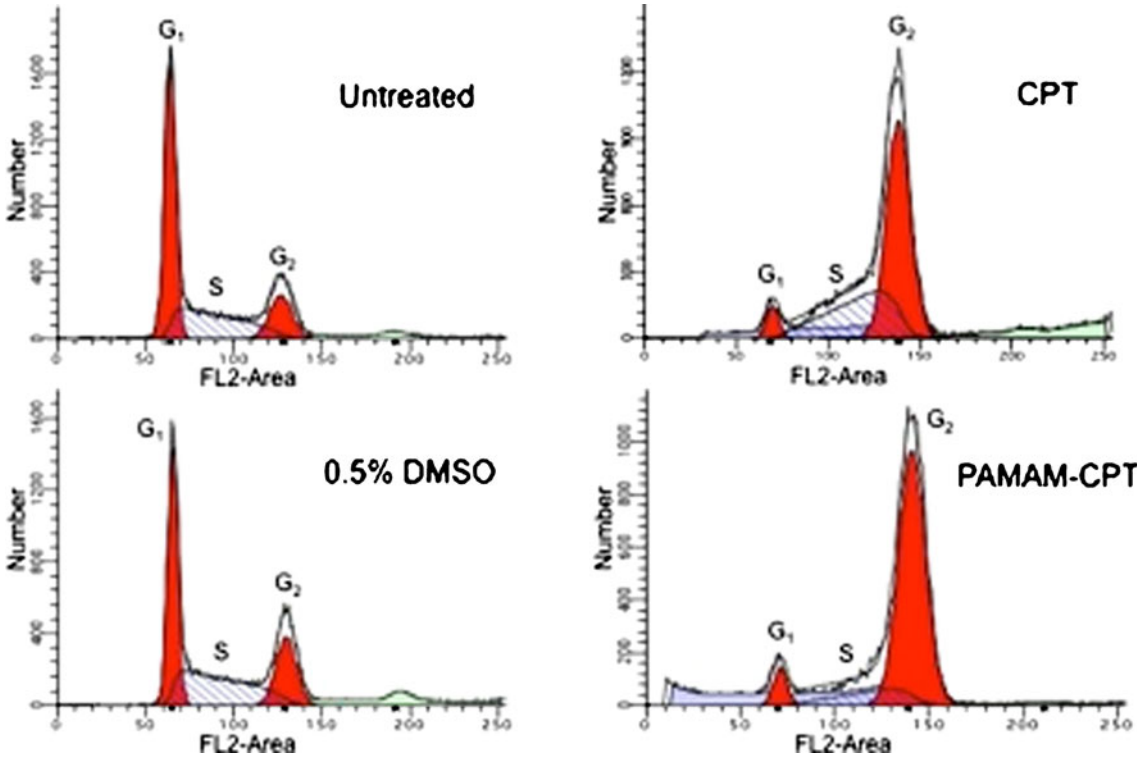

Fig. 3 Changes in DNA content of HCT-116 cells due to incubation with different forms of CPT. Cells were incubated with $3 \times IC_{50}$ concentrations of each drug for 24 h, fixed with ethanol and stained with propidium iodide. DNA content was measured by FACScan and data analyzed by ModFit software. Representative histograms from one experiment are shown.

free CPT. In conclusion, cytotoxic effect of the conjugate observed is not completely due to the released drug in media but also due to considerable amount of the conjugate that was internalized and consequently inhibited growth of HCT-116 cells.

Cell Cycle Analysis

Camptothecin (CPT) binds to the *topoisomerase* I-DNA covalent complex, resulting in a ternary complex, thereby stabilizing it. This prevents DNA relegation and therefore causes severe DNA damage. Damaged DNA prevents these cells from proceeding beyond the G_2 checkpoint in the cell cycle, resulting in accumulation of the cell population in the G_2 phase (33). Cell cycle arrest could be reversible when factors causing the arrest are removed, but if the damage is severe, then cell death cascades can be triggered.

Cell cycle experiments were performed on HCT-116 cells to study the effects of PAMAM-CPT treatment on cell cycle progression. Fig. 3 shows peaks depicting G_1, S and G_2 phases of the cell cycle for various treatments that were studied. Analysis of DNA content in HCT-116 cells showed that both CPT and PAMAM-CPT were effective in blocking the progression of cell cycle. A 0.5% DMSO control is also presented to confirm the fact that minute quantities of DMSO applied on cells, as a part of either CPT or PAMAM-CPT, does not affect the cell cycle progression. Untreated control HCT-116 cells had most of their cell population present in the G_1 phase (45%) and a relatively small number (16%) of cells in the G_2 phase. In contrast, cells treated with either form of CPT showed a significant accumulation in the G_2 phase (CPT—63%, PAMAM-CPT—68%, Fig. 4).

Cell population in the G_1 and G_2 phases of CPT and PAMAM-CPT treatments were statistically different from

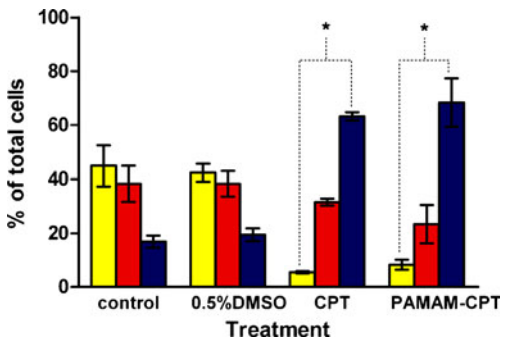

Fig. 4 Alteration of cell cycle distribution in HCT-116 cells after treatment with $3 \times IC_{50}$ concentrations of each analog. ■G_1; ■S; ■G_2. Cells were prepared, data acquired and analyzed as described in the legend of Fig. 3. Mean values±S.D. from three independent experiments are presented. Statistical comparisons between untreated and treated cells were performed. * indicates statistically significant data ($p < 0.05$).

the untreated control group (Fig. 4), indicating a pronounced accumulation of cells in the G_2 phase for these treatments when compared to G_1 phase. On the contrary, cells in S phase of PAMAM-CPT and CPT treatments were not significantly different from the untreated control group (Fig. 4), suggesting that the synthesis of DNA was not affected by these drugs which acted by blocking progression beyond the G_2 check point of the cell cycle.

Effects observed in both CPT and PAMAM-CPT treatments on cell cycle progression indicated that a similar mechanism was involved for both conjugated and free drug, causing the cell population to arrest in the G_2 phase. Several groups, including ours, previously reported that PAMAM dendrimers are endocytosed by the cellular machinery and are localized in lysosomes (34–36). Localization of PAMAM-CPT conjugate in lysosomes that include *esterases* and low pH (24) may cause the conjugate to break down, thereby releasing CPT. Once released, the drug should reach the nucleus and cause arrest of cells in G_2 phase comparable to free CPT.

Nuclear Fragmentation and Apoptotic Body Formation

Chemotherapeutic drugs, depending on extent of damage caused, can induce different modes of cell death (37–39). Cell death is a complex process that involves multiple independent and/or overlapping pathways that are not necessarily sequential events. Mammalian cells can die through different, biochemically and morphologically distinct pathways: apoptosis, autophagy, anoikis, cornification, necrosis and excitotoxicity represent a few modes of cell death (39,40). Mode of cell death also depends on the type of cells being studied. It was beyond the scope of this paper to investigate all individual pathways involved to ascertain mode of cell death induced by the conjugate. However,

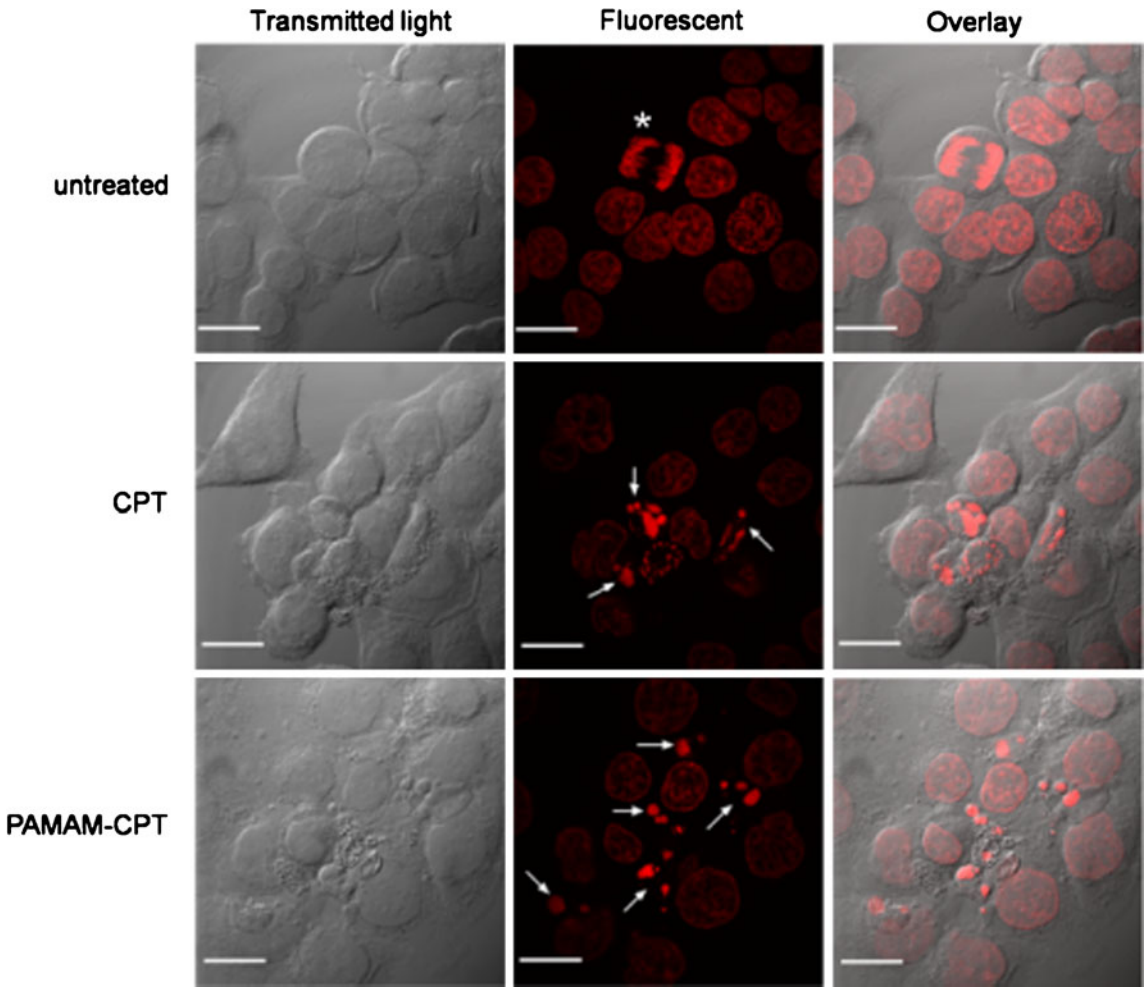

Fig. 5 Nuclear fragmentation and apoptotic body formation in HCT-116 cells due to CPT and PAMAM-CPT treatment. Cells were incubated with 3 × IC_{50} concentrations of CPT and PAMAM-CPT for 24 h, fixed and stained with DAPI. Cells were imaged using a confocal laser-scanning microscope Olympus FV1000. * indicates a cell undergoing mitosis in the untreated population. Arrows indicate apoptotic bodies. Bar in picture is 20 μm.

camptothecin and its analogs are known to induce apoptosis-mediated cell death as a result of severe DNA damage (41), and hence the morphological events accompanying apoptosis were studied for both CPT and PAMAM-CPT treatments.

The cell cycle arrest observed due to PAMAM-CPT treatment can trigger specific responses within the cell that may lead to apoptosis. Nuclear fragmentation is one of the morphological signs of apoptosis (42). In order to study the manifestations of apoptosis, such as nuclear fragmentation, treated cells were stained with DAPI, a nuclear dye (Fig. 5). Images of untreated cells showed normal, well-established cultures of HCT-116 containing a uniform, round, evenly stained and spread nucleus. A cell undergoing mitosis is also shown indicative of a healthy population of HCT-116 cells. On the contrary, no cells undergoing mitosis were observed in the PAMAM-CPT or CPT treatments, suggesting the inhibition of proliferation. Cells treated with either CPT or PAMAM-CPT showed many tiny, bright, rounded structures containing nuclear fragments as visualized by positive staining with DAPI. These structures, also named apoptotic bodies, are suggestive of apoptotic mode of cell death.

Onset of apoptosis is characterized by cell shrinkage and condensation of nuclear material followed by break-up of the nucleus (42). Subsequently, a process similar to budding takes place wherein smaller segments of crowded cellular organelles and nuclear fragments wrapped in plasma membrane form apoptotic bodies and detach from the original cell mass. It has been shown that proteolytic cleavage of key proteins by activated caspases can result in apoptotic morphology, and CPT class of drugs is associated with caspase-mediated apoptosis (41).

Polymeric systems may have a different fate inside the cell compared to the free drug, and it becomes imperative to delineate the mode of cell death. It is also important to understand whether conjugating a drug to a polymeric carrier alters the mechanism of action of the drug. It is evident from Fig. 5 that the PAMAM-CPT conjugate causes the nuclear material in HCT-116 cells to fragment, denoting signs of potential apoptosis similar to free drug (CPT).

Properties of the PAMAM-CPT conjugate observed *in vitro* are encouraging and lead us to the next stage of evaluating efficacy *in vivo* for treatment of colorectal cancers. Combined with their ability to translocate across epithelial barriers and target tumor sites, PAMAM-CPT conjugates have the potential to increase efficacy and reduce toxicity associated with CPT-based chemotherapy.

CONCLUSION

We report here the successful synthesis and characterization of a novel PAMAM-CPT conjugate. The nano-scale PAMAM-CPT conjugate displayed minimal release of drug in PBS and cell culture medium and was effective in inhibiting growth of colorectal carcinoma cells, HCT-116, *in vitro*. Cell cycle analyses revealed accumulation of large percentage of treated cells in the G_2 phase similar to free CPT treatment. In addition, PAMAM-CPT treatment led to nuclear fragmentation and formation of apoptotic bodies in HCT-116 cells. These results demonstrate the activity and potential of PAMAM-CPT conjugates as anti-cancer drug delivery systems.

ACKNOWLEDGEMENTS

This work was supported by a National Institutes of Health grant (R01-EB007470) and the Utah Science Technology and Research (USTAR) Initiative.

REFERENCES

1. Ulukan H, Swaan PW. Camptothecins: a review of their chemotherapeutic potential. Drugs. 2002;62:2039–57.
2. Li QY, Zu YG, Shi RZ, Yao LP. Review camptothecin: current perspectives. Curr Med Chem. 2006;13:2021–39.
3. Hatefi A, Amsden B. Camptothecin delivery methods. Pharm Res. 2002;19:1389–99.
4. Facts about cancer deaths. http://www.who.int/mediacentre/factsheets/fs297/en/, part of World Health Organization http://www.who.int/en/ (accessed 08/31 2009).
5. Current treatment options for colon cancer. http://www.cancer.gov/cancertopics/pdq/treatment/colon/Patient/page4, part of National Cancer Institute http://www.cancer.gov/ (accessed 08/31 2009).
6. Petrelli N. Surgical management of liver metastases from colorectal cancer. Clin Adv Hematol Oncol. 2006;4:673–5.
7. Duncan R. Polymer conjugates as anticancer nanomedicines. Nat Rev Cancer. 2006;6:688–701.
8. Matsumura Y, Maeda H. A new concept for macromolecular therapeutics in cancer chemotherapy: mechanism of tumoritropic accumulation of proteins and the antitumor agent smancs. Cancer Res. 1986;46:6387–92.
9. Najlah M, Freeman S, Attwood D, D'Emanuele A. Synthesis and assessment of first-generation polyamidoamine dendrimer prodrugs to enhance the cellular permeability of P-gp substrates. Bioconjug Chem. 2007;18:937–46.
10. Patri AK, Majoros IJ, Baker JR. Dendritic polymer macromolecular carriers for drug delivery. Curr Opin Chem Biol. 2002;6:466–71.
11. Tomalia DA, Reyna LA, Svenson S. Dendrimers as multi-purpose nanodevices for oncology drug delivery and diagnostic imaging. Biochem Soc Trans. 2007;35:61–7.
12. Svenson S. Dendrimers as versatile platform in drug delivery applications. Eur J Pharm Biopharm. 2009;71:445–62.
13. Kobayashi H, Brechbiel MW. Nano-sized MRI contrast agents with dendrimer cores. Adv Drug Deliv Rev. 2005;57:2271–86.
14. Malik N, Evagorou EG, Duncan R. Dendrimer-platinate: a novel approach to cancer chemotherapy. Anticancer Drugs. 1999;10:767–76.
15. Milhem OM, Myles C, McKeown NB, Attwood D, D'Emanuele A. Polyamidoamine Starburst dendrimers as solubility enhancers. Int J Pharm. 2000;197:239–41.

16. Kurtoglu YE, Mishra MK, Kannan S, Kannan RM. Drug release characteristics of PAMAM dendrimer-drug conjugates with different linkers. Int J Pharm. 2010;384:189–94.
17. Najlah M, Freeman S, Attwood D, D'Emanuele A. *In vitro* evaluation of dendrimer prodrugs for oral drug delivery. Int J Pharm. 2007;336:183–90.
18. El-Sayed M, Ginski M, Rhodes C, Ghandehari H. Transepithelial transport of poly(amidoamine) dendrimers across Caco-2 cell monolayers. J Control Release. 2002;81:355–65.
19. Jevprasesphant R, Penny J, Attwood D, McKeown NB, D'Emanuele A. Engineering of dendrimer surfaces to enhance transepithelial transport and reduce cytotoxicity. Pharm Res. 2003;20:1543–50.
20. Kolhatkar RB, Swaan P, Ghandehari H. Potential oral delivery of 7-ethyl-10-hydroxy-camptothecin (SN-38) using poly(amidoamine) dendrimers. Pharm Res. 2008;25:1723–9.
21. Greenwald RB, Pendri A, Conover CD, Lee C, Choe YH, Gilbert C, *et al.* Camptothecin-20-PEG ester transport forms: the effect of spacer groups on antitumor activity. Bioorg Med Chem. 1998;6:551–62.
22. Darzynkiewicz Z, Juan G, Bedner E. Determining cell cycle stages by flow cytometry. In: Bonifacino JS, Dasso M, Harford JB, Lippincott-Schwartz J, Yamada KM, editors. Current protocols in cell biology. New York: Wiley; 1999. p. 8.4.1–8.4.18.
23. Holt SJ. Some observations on the occurrence and nature of esterases in lysosomes. In: De Reuckand AVS, Cameron MP, editors. Lysosomes. London: Churchill; 1963. p. 114–25.
24. Liederer BM, Borchardt RT. Enzymes involved in the bioconversion of ester-based prodrugs. J Pharmaceut Sci. 2006;95:1177–95.
25. Bencharit S, Morton CL, Howard-Williams EL, Danks MK, Potter PM, Redinbo MR. Structural insights into CPT-11 activation by mammalian carboxylesterases. Nat Struct Biol. 2002;9:337–42.
26. Khatri VP, Petrelli NJ, Belghiti J. Extending the frontiers of surgical therapy for hepatic colorectal metastases: is there a limit? J Clin Oncol. 2005;23:8490–9.
27. Kitchens KM, Kolhatkar RB, Swaan PW, Eddington ND, Ghandehari H. Transport of poly(amidoamine) dendrimers across Caco-2 cell monolayers: influence of size, charge and fluorescent labeling. Pharm Res. 2006;23:2818–26.
28. Haag R, Kratz F. Polymer therapeutics: concepts and applications. Angew Chem Int Ed Engl. 2006;45:1198–215.
29. Singer JW, Bhatt R, Tulinsky J, Buhler KR, Heasley E, Klein P, *et al.* Water-soluble poly-(L-glutamic acid)-Gly-camptothecin conjugates enhance camptothecin stability and efficacy *in vivo*. J Control Release. 2001;74:243–7.
30. Pan H, Kopeckova P, Liu J, Wang D, Miller SC, Kopecek J. Stability in plasmas of various species of HPMA copolymer-PGE1 conjugates. Pharm Res. 2007;24:2270–80.
31. Najlah M, Freeman S, Attwood D, D'Emanuele A. Synthesis, characterization and stability of dendrimer prodrugs. Int J Pharm. 2006;308:175–82.
32. Xu H, Deng Y, Chen D, Hong W, Lu Y, Dong X. Esterase-catalyzed dePEGylation of pH-sensitive vesicles modified with cleavable PEG-lipid derivatives. J Control Release. 2008;130:238–45.
33. Tsao YP, D'Arpa P, Liu LF. The involvement of active DNA synthesis in camptothecin-induced G2 arrest: altered regulation of p34cdc2/cyclin B. Cancer Res. 1992;52:1823–9.
34. Kitchens KM, Foraker AB, Kolhatkar RB, Swaan PW, Ghandehari H. Endocytosis and interaction of poly (amidoamine) dendrimers with Caco-2 cells. Pharm Res. 2007;24:2138–45.
35. Saovapakhiran A, D'Emanuele A, Attwood D, Penny J. Surface modification of PAMAM dendrimers modulates the mechanism of cellular internalization. Bioconjug Chem. 2009;20:693–701.
36. Seib FP, Jones AT, Duncan R. Comparison of the endocytic properties of linear and branched PEIs, and cationic PAMAM dendrimers in B16f10 melanoma cells. J Control Release. 2007;117:291–300.
37. Green DR, Kroemer G. Pharmacological manipulation of cell death: clinical applications in sight? J Clin Invest. 2005;115:2610–7.
38. MacFarlane M. Cell death pathways–potential therapeutic targets. Xenobiotica. 2009;39:616–24.
39. Kroemer G, Galluzzi L, Vandenabeele P, Abrams J, Alnemri ES, Baehrecke EH, *et al.* Classification of cell death: recommendations of the Nomenclature Committee on Cell Death 2009. Cell Death Differ. 2009;16:3–11.
40. Galluzzi L, Maiuri MC, Vitale I, Zischka H, Castedo M, Zitvogel L, *et al.* Cell death modalities: classification and pathophysiological implications. Cell Death Differ. 2007;14:1237–43.
41. Shimizu T, Pommier Y. Camptothecin-induced apoptosis in p53-null human leukemia HL60 cells and their isolated nuclei: effects of the protease inhibitors Z-VAD-fmk and dichloroisocoumarin suggest an involvement of both caspases and serine proteases. Leukemia. 1997;11:1238–44.
42. Saraste A, Pulkki K. Morphologic and biochemical hallmarks of apoptosis. Cardiovasc Res. 2000;45:528–37.
43. Tomalia DA, Naylor AM, Goddard WA. Starburst dendrimers: molecular-level control of size, shape, surface chemistry, topology, and flexibility from atoms to macroscopic matter. Angewandte Chemie International Edition in English. 1990;29:138–75.